Pharmacophore-based Molecular Docking of Usnic Acid Derivatives to Discover Anti-viral drugs Against Influenza A Virus

Roney MIAH[1,2] (iD), Kelvin Wong Khai VOON[1,2], AKM Moyeenul HUQ[2,3*] (iD), Kamal RULLAH[4] (iD), Saiful Nizam TAJUDDIN[2] (iD), Hazrulrizawati Adb HAMID[1] (iD), Mohd Fadhlizil Fasihi Mohd ALUWI[1,2*] (iD)

[1] Faculty of Industrial Sciences and Technology, Universiti Malaysia Pahang, Lebuhraya Tun Razak, 26300 Gambang, Kuantan, Pahang Darul Makmur, Malaysia.
[2] Centre for Bio-aromatic Research, Universiti Malaysia Pahang, Lebuhraya Tun Razak, 26300 Gambang, Kuantan, Pahang Darul Makmur, Malaysia.
[3] School of Medicine, Department of Pharmacy, University of Asia Pacific, 74/A, Green Road, Dhaka, Bangladesh.
[4] Kulliyyah of Pharmacy, International Islamic University Malaysia (IIUM), Jalan Sultan Ahmad Shah, 25200 Kuantan, Pahang, Malaysia.
* Corresponding Authors. E-mail: moyeenul@ump.edu.my (AKMM. Huq); Tel. +60182620051.
fasihi@ump.edu.my (MFFM, Aluwi); Tel.+60129661942

ABSTRACT: For decades, influenza virus infection has been a serious health concern due to seasonal epidemics and pandemics, and it is continuing on the rise today, yet there is no gold-standard medication available for treating influenza viral infection. As a result, better influenza medicine is necessary to prevent illness. The purpose of this work was to investigate how effective usnic acid derivatives were as antiviral medications against the influenza virus in a computational approach. To discover the prospective medication as an anti-influenza agent, we employed pharmacophore-based molecular docking, ADMET, and drug-likeness studies, CYP isoform analysis and MD simulation approaches. Using pharmacophore filtering processes, twenty-three (23) usnic acid derivatives were acquired from an in-house database of 340 usnic acid derivatives. A docking simulation on the Influenza A H1N1 polymerase resulted in four molecules with a high affinity for the protein. The pharmacokinetics and drug-likeness predictions yielded two hit compounds, which were then subjected to cytochrome P450 enzyme screening to provide the lead molecule, denoted as compound-**4**. In addition, MD simulation of lead compound (Compound-4) was performed to verify the stability of the docked complex and the binding posture acquired in docking experiments. The findings revealed that compound-4 is a promising option for antiviral treatment of influenza illness in the future.

KEYWORDS: Influenza; Usnic acid; Pharmacophore; Molecular docking; MD Simulation.

1. INTRODUCTION

Influenza virus (IV) infection is a significant global health issue because of the serious sickness, mortality, and other causes that occur as a result of seasonal epidemics and pandemics [1]. Each year, seasonal human IV A infects over 20% of the worldwide population, resulting in a predicted three to five million serious cases and up to 650,000 fatalities; the most vulnerable are the elderly, children, and those with chronic conditions [2].

IV occurring among people is classified into three groups based on their internal proteins: A, B, and C. However, types A and B are mostly responsible for annual epidemics, while type C is less frequent and only triggers mild infections [3]. IV A viruses, which are also traditionally responsible for pandemics and cause the majority of IV infections, IAV is subject to regular genetic reassortment, which might lead to the emergence of new strains capable of triggering a global pandemic, as was the case with the novel H1N1 pandemic in 2009, which claimed the lives of over 284,000 people globally in the first year of the pandemic [4]. IV A is further subtyped based on the fusion of their surface glycoproteins, hemagglutinin (H or HA) and neuraminidase (N or NA) [5]. During the budding stage, the NA surface antigen is critical for releasing the virus from the host cell. Since its crystal structure was discovered, NA has been employed as a target protein for several therapeutic molecules. Oseltamivir is a licensed anti-influenza medication molecule that targets the H1N1 IV's

Miah et al.

**Pharmacophore-based Molecular Docking of Usnic Acid Derivatives
to Discover Anti-viral drugs Against Influenza A Virus**

Journal of Research in Pharmacy

Research Article

highly conserved NA active site, which has eight functional residues (R118, D151, R152, R224, E276, R292, R371, and Y406). Recent H1N1 outbreaks, as well as reports of oseltamivir-resistant strains, have demanded the development of potent anti-influenza medications [6]. Treatment of IV A infection is still limited, and the threat of a new pandemic from this infection still requires the development of the newest therapeutic agents. Therefore, it is necessary to develop a better drug to inhibit this virus.

Anti-IV medications are now licensed in two categories: (i) viral neuraminidase (NA) inhibitors like zanamivir and oseltamivir, and (ii) compounds that block the matrix-2 (M2) ion channel like amantadine and rimantadine [7]. The current drugs are ineffectual against the sudden appearance of new IV A subtypes, as seen during the 2009 pandemic, and they require annual updating and administration. Furthermore, these drugs provide only limited protection in elderly or immunocompromised subjects. Antiviral medicines are therefore an important alternative for preventing and treating dangerous IV infections, especially in frail people.

Usnic acid ($C_{18}H_{16}O_7$) (UA) is a secondary metabolite found in several lichen species. It has two enantiomers in (+)-and (-)-form and both enantiomers are effective against a large variety of gramme-positive bacterial strains [8]. It exhibits anti-viral [9], antibiotic [10], anti-fungicidal [11], analgesic [10], and other kinds of biological activity. Furthermore, UA has been demonstrated to have anti-mitotic effects on human cancer cell lines and to cause leukaemia, lung, and breast cancer cells to lose viable cells. Moreover, UA does not activate p53, and it has not been shown that it is implicated in DNA damage [12]. Antiviral properties of the UA have been discovered. The (+)-UA, which is commercially available, prevents the type 1 herpes virus from causing cytopathic effects. The Zn-UA complex medication was investigated as a papillomavirus treatment and was shown to suppress viral multiplication six months after treatment. (+)-UA inhibited Epstein–Barr virus replication at 1.0 g/ml (3 µM); (-)-UA was less active at 5.0 µg/ml (15 µM); and UA and its derivatives were also effective against the pandemic IV A (H1N1)pdm09 [9, 12]. As a result, this study used a series of computational-based approaches to discover anti-IV drug candidates based on the anti-viral and anti-IV A activity of UA derivatives, including pharmacophore-based virtual screening, molecular docking simulations, ADMET (absorption, distribution, metabolism, excretion and toxicity) prediction, drug-likeness properties, and CYP isoform analysis. Figure 1 depicts the detailed work plan.
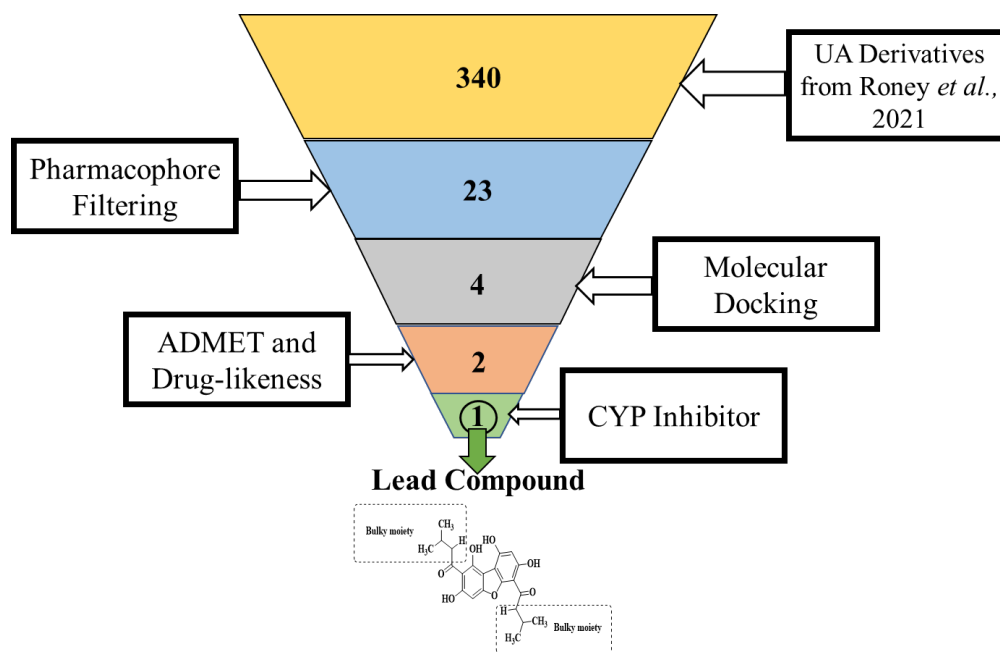

Figure 1. Virtual screening workflow to discover anti-Influenza A Virus.

Miah et al.

**Pharmacophore-based Molecular Docking of Usnic Acid Derivatives
to Discover Anti-viral drugs Against Influenza A Virus**

Journal of Research in Pharmacy

Research Article

2. RESULTS AND DISCUSSION

2.1. Pharmacophore Model Generation

Three *N*-terminal crystal protein structures of the polymerase acidic sub-unit of influenza virus were found (PDB ID: 4ZI0, 5FDD, and 5FDG). The co-crystallized compounds were selected to provide the pharmacophore characteristics (index No. 01 from 4ZI0, index No. 02 from 5FDD, and index No. 03 from 5FDG) (Table 1).

The "**Features Mapping**" was first utilized to produce 10 common features for each protein utilizing the co-crystallized protein compounds obtained. The "**BEST**" function and poling approach were then applied to produce up to 255 distinct conformations at 20 kcal/mol thresholds. The HipHop pharmacophore consolidated a total of 10 characteristics based on the rank value of every protein. Four features from 5FDG, four features from 4ZI0, and two features from 5FDD (of the same rank value, we chose the one above) have been selected based on the highest rank value. The top ten pharmacophore hypotheses were split into 3 pharmacophore-based groups by HHHDDAA (01, 02, 03, 04), HHDDD (05, 06, 07, 08), HHHDA (09), and HHHAA (10). In these three groups, hypotheses were identified by the direction of the hydrogen bond vectors, the location of characteristics, or both (Table 2). Figure 2 shows the workflow.
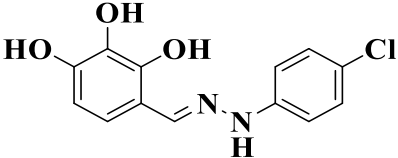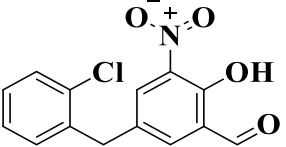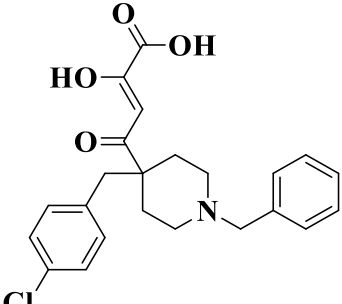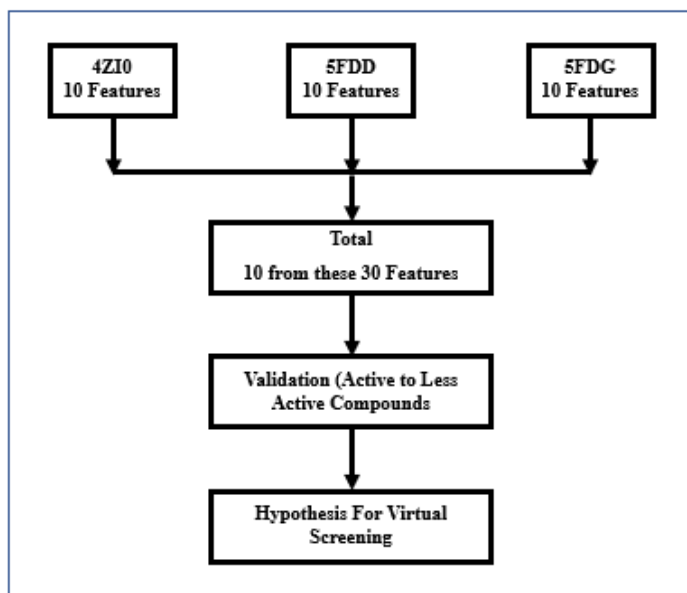

Figure 2. Pharmacophore model generation, validation, and virtual screening workflow for Influenza A Virus.

1023

Miah et al.

**Pharmacophore-based Molecular Docking of Usnic Acid Derivatives
to Discover Anti-viral drugs Against Influenza A Virus**

Journal of Research in Pharmacy

Research Article

Table 1. Activities of inhibitors of Influenza A Virus (Fudo et al., 2016).

Index Number	Structure	PDB	IC$_{50}$ Value
01		4ZI0	-
02		5FDD	-
03		5FDG	0.43

Notes: IC$_{50}$ values were calculated according to the relevant literature.

Notes: IC$_{50}$ values were calculated according to the relevant literature.
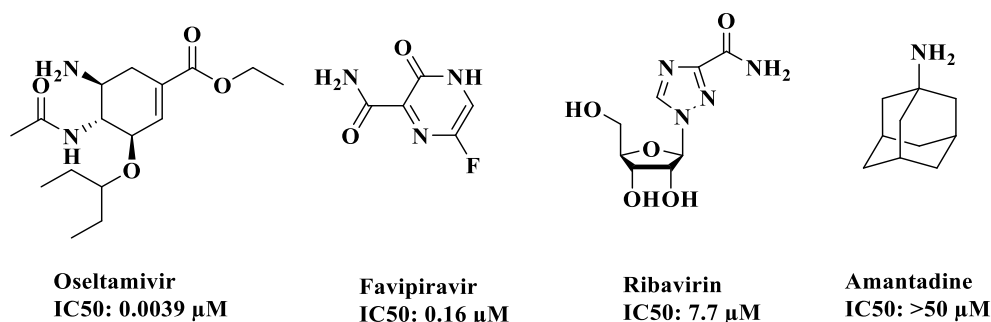
Table 2. Chemical features of the ten hypotheses generated from the three active compounds from three proteins for Influenza A virus (4ZI0, 5FDD and 5FDG).

| Hypothesis	Feature	PDB ID	Rank	Max Fit
01	HHHHDDA	5FDG	16.509	7
02	HHHHDDA	5FDG	16.483	7
03	HHHHDDA	5FDG	16.440	7
04	HHHHDDA	5FDG	16.430	7
05	HHDDD	4ZI0	12.133	5
06	HHDDD	4ZI0	12.114	5
07	HHDDD	4ZI0	12.086	5
08	HHDDD	4ZI0	12.081	5
09	HHHDA	5FDD	10.109	5
10	HHHAA	5FDD	9.909	5

Notes: H denotes a hydrophobic group, D denotes a hydrogen bond donor, and A denotes a hydrogen bond acceptor. (b) The compound ranking score from the training set that best fits the hypothesis. The higher the rank, the less probable it is that the compounds in the training set have a probability relationship with the hypothesis. The best hypothesis is the most valuable hypothesis.

Miah et al.

Pharmacophore-based Molecular Docking of Usnic Acid Derivatives to Discover Anti-viral drugs Against Influenza A Virus

Journal of Research in Pharmacy

Research Article

2.2. Validation of Pharmacophore Model

The most acceptable pharmacophore model was chosen from 10 pharmacophore hypotheses produced using the approach described by Liu *et al.*, 2020. A test set of IV inhibitors ranging in activity from more active to less active was picked from a variety of sources to create a test set (Figure 3). The substances in the test set corresponded to each of the 10 hypotheses, and the results were shown on a heatmap (Figure 4 C). The heatmaps revealed that hypothesis 10 (HHHAA) was the most appropriate of the ten pharmacophore hypotheses (Figure 4 B). As shown in Figure 4 A, a1 and a2 were involved with the carbonyl (=O) group and the nitro (-NO2) group. The b1 and b3 features were defined by the phenyl group, and the b2 features involved the halogen (Cl).

Oseltamivir
IC50: 0.0039 μM

Favipiravir
IC50: 0.16 μM

Ribavirin
IC50: 7.7 μM

Amantadine
IC50: >50 μM

Figure 3. The Test Set (More Active to Less Active) for Pharmacophore Model Validation of Influenza A Virus.
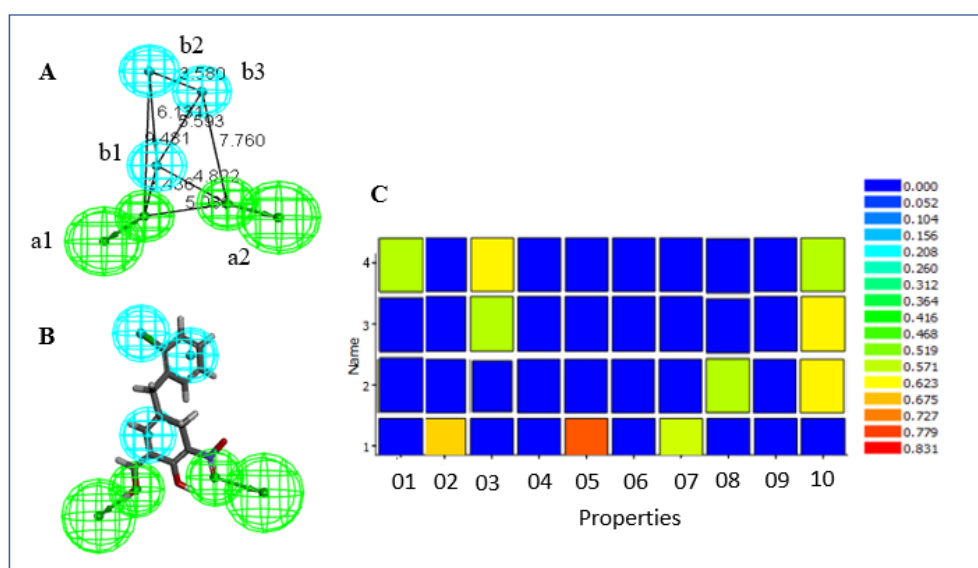
Figure 4. HipHop pharmacophore Generation. **(A)** The HipHop-Hypo10. The color of the pharmacophore features, namely, HBA and H are green and blue, respectively. **(B)** HipHop-Hypo10 chemical features. **(C)** The heat map of the 10 hypotheses in the test.

2.3. Pharmacophore-based Virtual Screening

In the in-house database, 340 UA derivatives were practically tested using the prior model, HipHop-Hypo10. Twenty-three (23) compounds were chosen based on a fit value of ≥3.6 from the pharmacophore filtering and then carried out in a molecular docking procedure (Table S2).

2.4. Molecular Docking with Selected Compounds

Molecular docking is a computer tool that helps researchers better understand how proteins interact with their ligands. The native location, orientation, and conformation of ligands that bind to the active region of the target protein are predicted using this approach [13]. The crystal structure of IV A virus neuraminidase

1025

Miah et al.
Pharmacophore-based Molecular Docking of Usnic Acid Derivatives to Discover Anti-viral drugs Against Influenza A Virus

Journal of Research in Pharmacy

Research Article

in complex with 5-(2-chlorobenzyl)-2-hydroxy-3-nitrobenzaldehyde (PDB ID: 5FDD) [14] was acquired from the Protein Data Bank (www.rcsb.org). The crystal structure consists of four chains (A, B, C, and D), with all four chains being used. Using the DS3.1, the co-factor and water molecules were eliminated, and hydrogen was added. In the current work, pharmacophore screening yielded 23 compounds, which were then molecular docked with IV A H1N1 polymerase (PDB ID: 5FDD). In addition, the DS3.1 programme was utilized to examine the precise interactions of the best compounds that bind well to the active region with both bonded and non-bonded interactions. These compounds had a lower binding energy than the reference molecule (co-crystallized ligand), indicating that they bind to the active site of NA more effectively. According to the molecular docking studies, all 23 compounds had a stronger binding relationship than the co-crystallized ligand.

Compound-**4** was shown to have the highest binding affinity for creating a ligand-protein complex with H1N1 polymerase, with a binding interaction of-54.6676 kcal/mol. The output of the molecular docking simulation may be used to see the molecular interaction between the ligand and the binding site of H1N1 polymerase. During the creation of the ligand-protein complex, compound-**4** interacted with six amino acid residues, forming three hydrogen bonds with Leu91, Tyr29, and Glu104 (Figure 5B). Compound-**133**, which came after compound-**4**, performed well in complex binding with H1N1 polymerase (binding interaction of -52.2823 kcal/mol). The compound-**133** made two hydrogen bridges with Tyr29 and Lys122 and interacted with eight amino acid residues (Figure S1). The binding affinity of compounds-**140** and compounds-**185** was 55.5848 and 52.4477 kcal/mol, respectively. Compound-**140** was also discovered to establish hydrogen bonds with Tyr29, Lys39, Leu91, and Arg109 residues (Figure S2). Furthermore, molecule-**185** was shown to mediate hydrogen bonds with Glu65, Arg69, and Leu91 residues (Figure S3).

Furthermore, all of these compounds have an RMSD value of less than 2.0 Å, indicating that all ligand poses generated during docking simulations were verified and accurately reflected the basic ligand-protein interactions in real time. On the other hand, as previously indicated, the four best ligands interacted with the critical residues on the IV H1N1 polymerase.
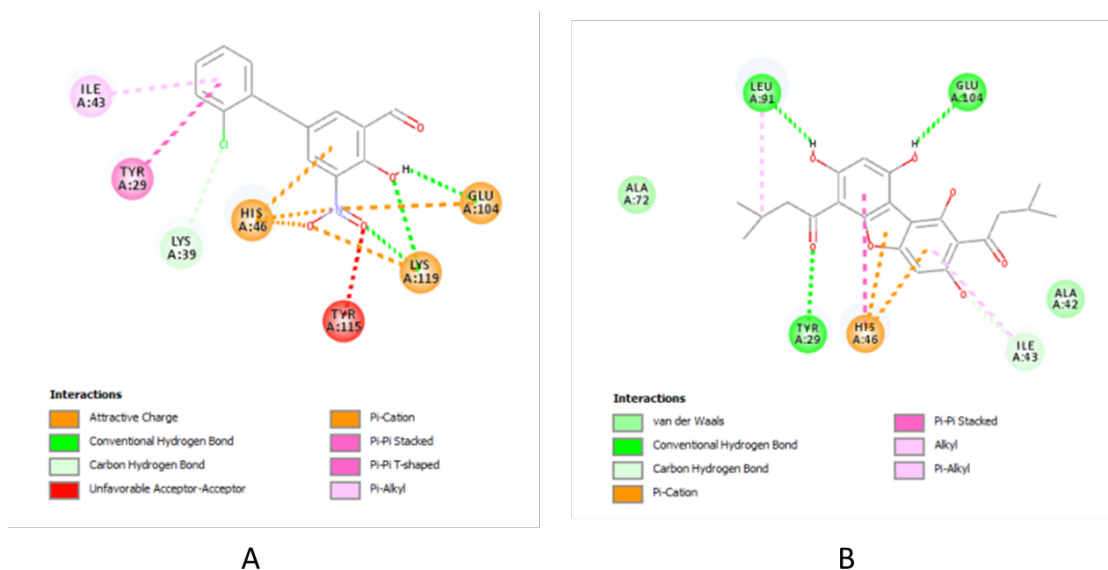
Figure 5. Molecular docking interaction analysis of (A) co-crystallized ligand and (B) Lead compound (compound-**4**) with Influenza A (5FDD).

2.5. ADMET Prediction

It would be advantageous to resolve issues that might result in lead compound loss in preclinical and clinical studies, such as poor pharmacokinetic profiles and hazardous consequences. From a cost standpoint, using in-silico methods to estimate the likely pharmacokinetic characteristics and toxicity of the hit compounds would be advantageous. The four compounds acquired following molecular docking (**4**, **133**, **140**, and **185**) were then exposed to ADMET modules.

ADMET experiments in DS3.1 were used to evaluate compounds (**4**, **133**, **140**, and **185**), and the exact results are presented in Table 4. All ligands are deemed drug candidates for future ADMET investigation

Miah et al.
Pharmacophore-based Molecular Docking of Usnic Acid Derivatives to Discover Anti-viral drugs Against Influenza A Virus

Journal of Research in Pharmacy

Research Article

based on these criteria, with the standard value compared to the co-crystallized ligand. Human intestinal absorption (HIA), aqueous solubility, blood brain barrier (BBB) penetration, plasma protein barrier (PPB) penetration, and hepatotoxicity are among the expected ADMET characteristics.

According to the ADMET prediction findings examined with the value of >150, three substances were assessed to be efficiently eaten in the human gut. Table 3 shows that the chosen compounds and the reference (co-crystallized ligand) compound both exhibit positive human intestinal absorption (HIA+), indicating that they are easily absorbed in the human intestine. Compounds **4**, **133**, and **185** with the vanillin moiety, in particular, exhibited a capable logarithm of the molar solubility value range of -5.398 to -5.006, respectively. These compounds, like co-crystallized ligand, have good aqueous solubility, whereas compound-**140** has poor solubility, resulting in better absorption and distribution properties for the selected compounds and the reference (co-crystallized ligand) compound. Only compound-**4** was predicted to have a plasma protein binding of ≥90%. The plasma protein binding (PPB) model suggests if a drug will be substantially bound to blood carrier proteins (≥90% bound) [15], and the better compound binds to the plasma protein, then consider that compound as a better drug. The permeability of the Blood-Brain Barrier was predicted to be quite high for all of the drugs (BBB). Depending on where a medicine must be targeted and its toxicity profile, crossing the BBB might be useful or detrimental [16]. In the BBB-plot, all substances lie outside of a very high Blood-Brain Barrier permeability, suggesting that they can traverse BBB and hence pose no risk of nervous system toxicity. This programme was also used to predict the hepatotoxicity potential of the chosen ligands. All of the chemicals were discovered to have a hepatotoxic profile, which implies they might cause liver damage.

Table 3. ADMET analysis of the compounds.

Compound Number	HIA					BBB		PPB	Hep
	PSA[a]	ALogP98[b]	Level[c]	Log(Sw)[d]	Level[e]	LogBB[f]	Level[g]	Prediction[h]	Prediction[i]
4	130.41	4.59	2	-5.00	2	0	4	1	1
133	120.32	4.17	2	-5.24	2	0	4	0	1
140	144.09	4.16	2	-7.10	1	0	4	0	1
185	168.44	3.10	3	-5.39	2	0	4	0	1
Co-crystallized ligand	80.93	3.88	0	-4.52	2	-0.23	2	1	1

HIA: Human Intestinal Absorption, AS: Aqueous Solubility, BBB: Blood Brain Barrier Penetration, PPB: Plasma Protein Binding, Hep.: Hepatotoxicity

[a]Polar surface area (PSA) of more than 150 (extremely low absorption).
[b]Log P (Alog P98) depending on atoms (≤2.0 or P ≥ 0: extremely low absorption).
[c]Estimation of human intestine absorption level: 0 (excellent), 1 (moderate), 2 (low), 3 (very low).
[d]The molar solubility log (Sw) based 10logarithm (25oC, pH = 7.0) (suitable drug-like substances: 6 <log(Sw) ≤ 0).
[e]Estimated level of water solubility; 0 (extremely low), 1 (very low), 2 (low), 3 (good), 4 (optimal), 5 (too soluble), 6 (warning: molecules with one or more unknown Alog P calculation).
[f]Extremely strong penetrants (log BBP ≥ 7)
[g]Estimation of the Level blood brain barrier penetration: 0 (extremely high penetration), 1 (strong), 2 (moderate), 3 (poor), 4 (extremely poor penetration) (undefined).
[h]Estimation of Plasma-protein binding (0: <90 %; 1: ≥90 %).
[i]Estimatopn of Inhibition of the cytochrome P450 2D6 enzyme (0: non-inhibitor; 1: inhibitor).
[j]Estimation of Hepatotoxicity (0: non-toxic; 1: toxic).

2.6. Drug-likeness Properties

In the early stages of drug development, drug-likeness analysis is critical. Lipinski's rule of five (RO5) states that a drug-like molecule must have a molecular weight (MW) of 500 Da, five hydrogen bond donors (HBDs), ten hydrogen bond acceptors (HBAs), and a topological polar surface area (TPSA) of less than 140 Å^2, with only one number of violations permitted [17].

According to Table 4, only compounds **4** and **133** showed a decent chance of excellent absorption, with logP values of 5.12 and 4.70 respectively, among four compounds (**4**, **133**, **140**, and **185**) where the acceptable range is ≥5. The TPSA values of compounds **4** and **133** were determined to be 128.19 Å^2 and 119.37 Å^2, respectively, which were both less than 140 Å^2, indicating that both compounds were acceptable. Despite the fact that compounds **4** and **133** have a smaller range of rotatable bonds (1) <10, they have limited conformational flexibility. Furthermore, the compounds **4** and **133** have low molecular weights of 400.43 and

Miah et al.

**Pharmacophore-based Molecular Docking of Usnic Acid Derivatives
to Discover Anti-viral drugs Against Influenza A Virus**

Journal of Research in Pharmacy

Research Article

504.54 g/mol, respectively, due to the presence of seven and eight hydrogen bond acceptors (nON) below ten and four and two hydrogen bond donors (nONH) below five. Finally, within the 20-70 range, compounds **4** and **133** contain 29 and 37 atoms, respectively. Only compounds **4** and **133** were determined to meet Lipinski's criteria after a thorough examination of the data.

Table 4. Drug-likeness Properties of Best Compounds for Influenza A Virus

Compound Number	MiLogP	TPSA	n. A.	MW	n ON	n ONH	n. V.	n. R.	Vol
4	5.12	128.19	29	400.43	7	4	1	6	357.14
133	4.70	119.37	37	504.54	8	2	1	6	444.48
140	4.02	141.36	41	586.44	8	4	1	7	449.02
185	1.55	166.02	39	530.53	10	5	1	6	455.33

Milog P: segregation constant ≤5

TPSA: Topological polar surface area ≥140Å²

nA: atomic number 20 - 70

MW: molecular weight ≤500

nON: number of hydrogen-bonds acceptor ≤10

2.7. CYP Isoform Study

The biotransformation of numerous xenobiotics in the human body requires cytochrome P450 (CYP450) enzymes. Although there are more than fifty isoforms of this enzyme family, CYP1A2, CYP2C9, CYP2C19, CYP2D6, CYP3A4, and CYP3A5 are commonly regarded the most important CYP450 enzymes since they metabolize 90% of medications [13]. The CYP3A4 isoform, which is connected in 50% of the drug's metabolism and has an intestine and kidney, is the first and most important isoform [18]. Moreover, the isoforms CYP2C9, CYP2C19 and CYP1A2 are active in 15%, 12% and 11% of drug metabolism, respectively [19]. The cytochrome P450 mixed-function oxidase system, which includes CYP1A2, is involved in the human body's xenobiotic metabolism [20]. The CYP2C9 gene codes for an enzyme located in the endoplasmic reticulum, a cell structure involved in protein processing and transportation [21]. Compounds including steroid hormones and fatty acids are broken down (metabolized) by the CYP2C9 enzyme. The CYP2C9 enzyme is also involved in the breakdown of warfarin, a medicine that thins the blood and prevents blood clots. This enzyme also aids in the metabolism of other anti-inflammatory medications like ibuprofen [22]. Profiling the drug candidate's interaction with these enzymes is critical for determining if the drug might cause toxicities or interact with another drug in the body, resulting in a pharmacological effect that is ineffectual [23]. The activity of this enzyme's metabolism is reduced by a CYP450 inhibitor [24]. It's critical to determine if the medication candidate at issue can inhibit a specific isoform of the CYP enzyme. Good medication is defined as drugs that do not become opponents of all CYP isoforms [25]. Inhibitors have the potential to harm an enzyme's metabolic capacity. Compound-**4** results in a negative value for the CYP2C19, CYP2D6, and CYP3A4 isoforms. Table 5 contains the summary data. The CYP2C19 gene codes for an enzyme that is found mostly in liver cells in the endoplasmic reticulum, a cell structure that is involved in protein processing and transport [26]. Many medicines that effect on the central nervous system, such as antidepressants, antipsychotics, and central opioids, are metabolized by CYP2D6. This enzyme is encoded by a polymorphic gene, with 7% of Caucasians ('low metabolizers') displaying no enzymatic activity [27]. CYP3A4 is a vital enzyme in the body that is mostly present in the liver and gut. It oxidizes tiny foreign organic molecules (xenobiotics), such as poisons or medications, so they may be eliminated from the body [25].

Miah et al.
**Pharmacophore-based Molecular Docking of Usnic Acid Derivatives
to Discover Anti-viral drugs Against Influenza A Virus**

Journal of Research in Pharmacy

Research Article

Table 5. CYP Inhibitor od Best Compound for Influenza A Virus

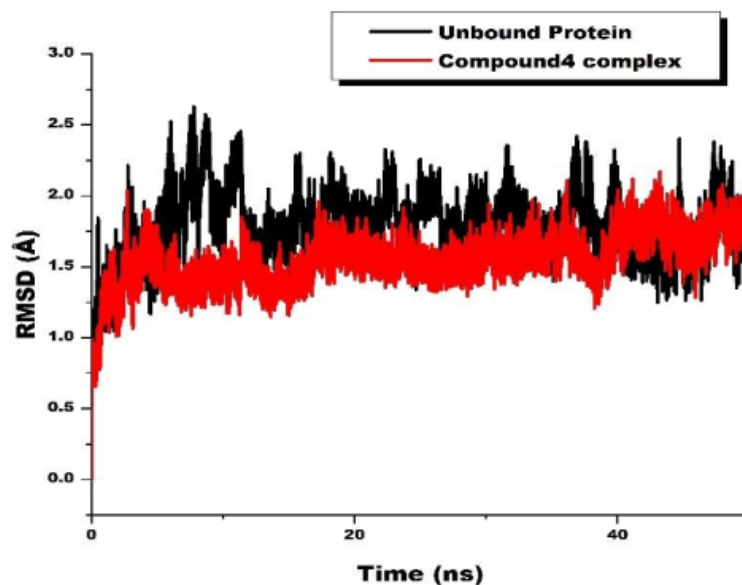| Compound Number	Inhibitor					Log K_P (skin permeation)
	CYP1A2	CYP2C19	CYP2C9	CYP2D6	CYP3A4	
4	Yes	No	Yes	No	No	-5.02 cm/s
133	No	Yes	Yes	No	Yes	-6.23 cm/s
Co-crystallized ligand	Yes	Yes	Yes	No	No	-5.27 cm/s

No= non-inhibitor; Yes= inhibitor

2.8. Molecular Dynamic (MD) Simulation

Through a 50 ns classical MD simulation analysis, the stability of the complexes between IV A and the final small molecule (Compound-4) was investigated. To investigate the dynamic behavior of the molecules, many metrics were extracted from either the MD simulation trajectories of every complex, including the RMSD, RMSF, RoG, and intermolecular hydrogen bonds. Table 7 shows the average, maximum, and lowest values of RMSD, RMSF, and RoG.

Table 6. Average, maximum and minimum protein-RMSD, ligand-RMSD, protein-RMSF, ligand-RMSF and RoG

Complex	Protein RMSD	Ligand bound RMSD	Protein RMSF	Ligand bound RMSF	Protein RoG	Ligand bound RoG
Average	1.85 Å	1.4 Å	15.5 Å	7.25 Å	16.05 Å	16.4 Å
Maximum	2.7 Å	2.1 Å	26 Å	12.5 Å	16.6 Å	16.7 Å
Minimum	1.0 Å	0.7 Å	5 Å	2 Å	15.5 Å	16.1 Å

The stability of protein-ligand complex was determined using the protein backbone RMSD computed from the MD simulation trajectory. The greater the RMSD, the more likely the protein is to be unfolded, and the lower the RMSD, the more likely the protein is to be folded. The system equilibration is defined by a low fluctuation or constant variation in RMSD. Each frame's backbone RMSD was determined and is shown in Figure 6. As shown in Figure 6, the protein backbone RMSD was steadily raised up to around 16 ns, and then reached equilibration until the simulation ended. There were no abnormal or atypical backbone deviations discovered. The average RMSD of the backbone may be used to estimate the protein's deviation during MD simulation. When attached to Compound-4, the backbone average RMSD was determined to be 1.85 Å which is considered perfectly fine for small and globular protein [28]. The protein-ligand combination was clearly stable during the simulation, as seen by the low RMSD and continuous variation.

Miah et al.

**Pharmacophore-based Molecular Docking of Usnic Acid Derivatives
to Discover Anti-viral drugs Against Influenza A Virus**

Journal of Research in Pharmacy

Research Article

Figure 6. Influenza A backbone RMSD bound with compound-4

During the MD simulation, it's crucial to keep an eye on the ligand's divergence from its natural structure. Compound-4 was found to be nearly constant throughout the experiment. Compound-4 showed a little variation, which might be attributable to the molecule's orientational shift. The maximum ligand RMSD was discovered to be 1.4 Å for compound-4, as shown in Table 6. In the same plot, it was observed that the ligand RMSD was not significantly larger than the protein RMSD which indicates that ligand does not diffuses away from the initial binding site.

The amino acid residues of protein molecules serve a key role in achieving the stability of complex. The RMSF parameter may be used to investigate the variability of individual amino acid residues. The RMSF of all IV A amino acids was calculated using MD simulation trajectories, and the results are shown in Figure 7. IV A amino acids were shown to differ in a similar way when attached to compound-4. The difference between the highest and average RMSF might provide insight into simulation variation. When IV A was bonded with compound-4, the aforementioned value was determined to be 7.5 Å which maintained a stable RMSF value over time [29]. According to Aldahham et al. [30], the above data clearly substantiated the low fluctuation of the amino acid residues in the dynamic states. The limited variation of amino acid residues in dynamic situations was clearly demonstrated by the above data.
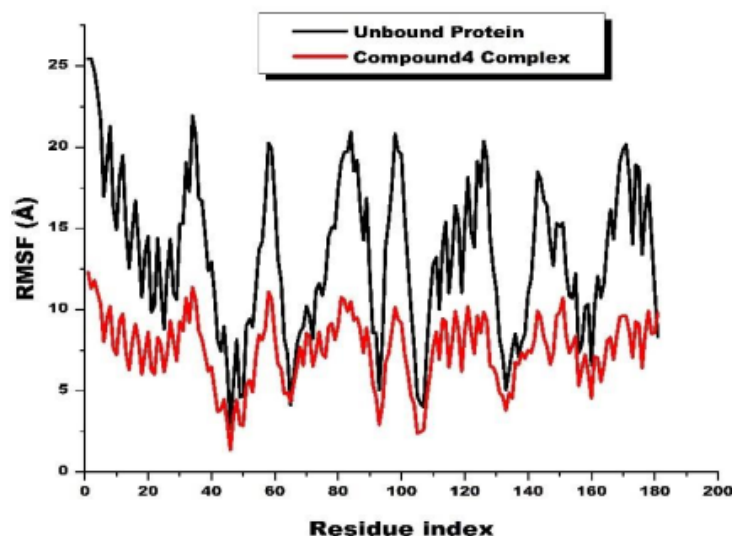
1030

Miah et al.

**Pharmacophore-based Molecular Docking of Usnic Acid Derivatives
to Discover Anti-viral drugs Against Influenza A Virus**

Journal of Research in Pharmacy

Research Article

Figure 7. RMSF of amino acid residues of Influenza A bound with compound-4

The RoG, computed from the MD simulation trajectory, was used to investigate the compactness of IV A bound with compound-4. Each system's RoG was calculated and is shown in Figure 8. Surprisingly, the entire system remained compact throughout the experiment. Throughout the experiment, there was not a single complex with an unexpected departure. The difference in RoG values between the greatest and lowest IV A binding with compound-4 was determined to be 0.35 Å. It is quite interesting that proposed molecular system ow deviation and compactness explained the rigidity and stability of the complexes [30]. It's fascinating that the suggested molecular systems maintained their compactness in the same way that the co-crystallized ligand did. The stiffness and stability of the complexes were explained by minimal deviation and compactness.
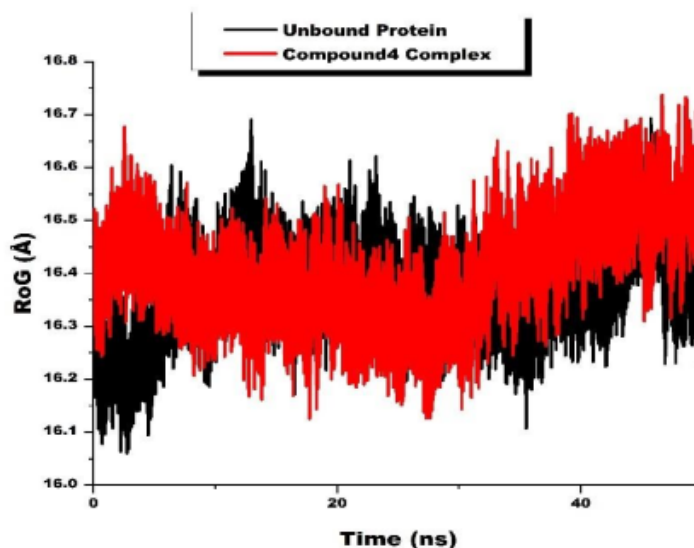

Figure 8. The radius of gyration of Influenza A bound with compound-**4**

Throughout the simulation, protein interactions with the ligand were detected. Understanding the stability of the projected protein–ligand combination requires H-bond interaction analysis (Figure 9). The ligand's ability to fit into the binding site is aided by H-bonding. Tyr29, Glu65, Asp93, Gly104, Gly106, Val107, and Tyr115 demonstrated H-bond interaction with Compound-4. With Tyr29 and Glu104, compound-4

1031

formed an H-bond. These residues participating in interactions with ligand indicating that it was highly stable throughout the simulation. In docking investigations, comparable interactions were detected as well.
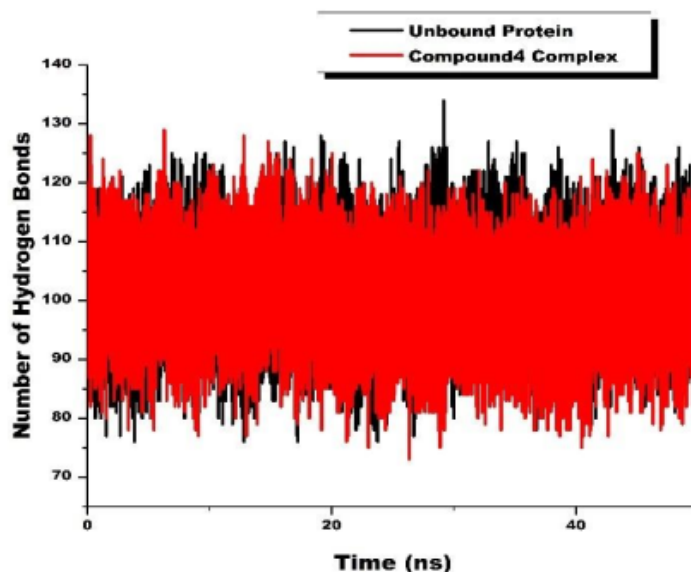
Figure 9. Number of Hydrogen bonds of Influenza A bound with compound-4

In a nutshell, the lead compound-**4** was found to bear a bulky moiety (Figure 10). It has been reported that bulky moieties such as prenylated moiety demonstrate strong antiviral activity against the IV. For instance, the compound containing the prenyl moiety, Elsholtzioxin, showed anti-IV efficacy against strain A/WSN/33/2009 (H1N1) with a 47.19% inhibition rate [31]. It is also supported by the discovery that compound-**4**, which contains a bulky bearing moiety, may play an important role in influenza A inhibition activity.
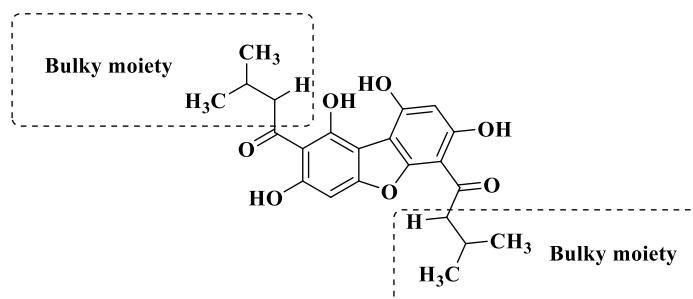
Figure 10. Lead Compound (Compound-**4**) as Potential anti-Influenza A Virus.

In summary, the lead compound (Compound-**4**) was shown to have a good fit value of 3.71868. From the docking result, compound-**4** has also been found to have a strong binding affinity to the *N*-terminal region of the influenza strain H1N1 polymerase acidic subunit with a binding energy of -54.6676 kcal/mol. Furthermore, based on the interaction analysis, compound-**4** established three hydrogen bonds with the residues Leu91, Tyr29, and Glu104 and one hydrophobic contact with the residue Ile43. The lead compound-4's drug-likeness and ADMET properties were both satisfactory. The interaction of a drug candidate with P450 (CYP450) enzymes is essential for evaluating whether the drug will induce toxicities or interact with another medication in the body, resulting in a pharmacological effect with no inhibitor to CYP2C19, CYP2D6 and CYP3A4 isoforms.

Miah et al.

**Pharmacophore-based Molecular Docking of Usnic Acid Derivatives
to Discover Anti-viral drugs Against Influenza A Virus**

Journal of Research in Pharmacy

Research Article

3. CONCLUSION

According to the computational analysis, the current study was able to uncover a unique and useful chemical with a strong binding attraction to IV A. Furthermore, the projected high negative binding energy values of these drugs support our hypothesis that they have the potential to block IV A. The information gathered from this study will be extremely useful in improving the identification of IVA target-specific therapeutic compounds. The current study also shows that the NA enzyme of H1N1 is a viable therapeutic target for the anti-IV A properties of the currently examined compounds. On the basis of ADMET prediction, drug profiling, and CYP isoform analysis, the current computational investigations explore compound-4 has the potential to be a viable and successful anti-IV A drug. Furthermore, MD simulations for 50 ns revealed that the ligand interactions with the residues of IV A are part of the essential residues for structural stability and functionality. The findings will be beneficial since they will give insight into the efficacy of a drug when compared to a reference co-crystallized ligand before chemical and biological tests are carried out.

4. MATERIALS AND METHODS

4.1. Data Collection and Preparation

To develop common feature-based pharmacophore models, three structurally different co-crystallized ligands, active against IV A from three proteins (PDB codes: 5FDG, 5FDD, and 4ZI0), were utilized as the training set. Table 1 lists the molecular characteristics of these compounds. The test set consisted of four compounds, ranging from the most active to the least active, IV A (Figure 3). The Discovery Studio (DS3.1) was used to prepare and optimize all of the compound.

4.2. Pharmacophore Model Generation

Three anti-IV A co-crystallized ligands from three target proteins with the PDB codes 5FDG, 5FDD, and 4ZI0 were utilized to construct HipHop pharmacophore models (Table 1). In this study, the co-crystallized ligands of target proteins were selected as the training set of compounds randomly. For all ligands, the primary value was set to 2 and the maximum-omit feature was set to 0. The pharmacophore module "**Feature Mapping**" was utilized to identify the relevant chemical attributes of the training set compounds before constructing the HipHop pharmacophore model. Subsequently, as building components for the pharmacophore model, hydrogen bond acceptor (HBA), hydrogen bond donor (HBD), hydrophobic feature (HC), hydrophobic aliphatic (HAL), hydrophobic aromatic (HAR), positive ionizable (PI), and aromatic ring (AR) were chosen. The "**BEST**" algorithm was used to develop 255 conformations under a 20 kcal/mol energy barrier in order to get a varied set of conformations. Table 2 lists and ranks the derived pharmacophore models with significant common chemical features.

4.3. Validation of Pharmacophore Model

On the basis of the fit findings acquired with test sets, the hypothesis regarding pharmacophore is verified. The test sets (Figure 3), which range from the most active to the least active chemicals, were prepared following a similar process as the training set [32]. In this study, the test set of compounds was selected based on the IC_{50} value (0.0039 to ≤50 μM). The hypothesis was then tested utilizing the "**Ligand Profiler module**" to investigate if the Fit Value could be used to determine the active compounds.

4.4. Pharmacophore-based Virtual Screening

The validated pharmacophore model HipHop-Hypo10 was utilized to screen 340 UA derivatives, which were obtained from our previous publication [19]. All of these compounds were optimized in DS3.1, with HipHop-Hypo10 being employed to screen compounds utilizing "**Screen Library module**" in DS3.1. The number of conformations was set to 255 while the conformation technique was set to BEST. The rest of the parameters were left at their default settings. Lastly, the selected pharmacophore hypothesis was linked to specific chemical compounds that were linked to the structure activity relationship (SAR) [33].

Miah et al.

**Pharmacophore-based Molecular Docking of Usnic Acid Derivatives
to Discover Anti-viral drugs Against Influenza A Virus**

Journal of Research in Pharmacy

Research Article

4.5. Protein Preparation

The crystallized structure of the target protein was downloaded from the Protein Data Bank (https://www.rcsb.org/) with the PDB code 5FDD [14]. This protein entry is the crystallized structure of the N-Terminal Region of Influenza Virus Polymerase Acidic, which co-crystallized with an inhibitor called (2Z)-4-[1-benzyl-4-(4-chlorobenzyl) piperidin-4-yl]2-hydroxy-4-oxobut-2-enoic acid. In order to prepare for the next steps, the structure was cleaned. Inserting the missing amino acid residues and removing substitute conformations, removing water and ligand molecules, adding missing loop regions, optimization of loop regions using the CDOCKER algorithm, minimization of loop regions, and protonation of the structure were all part of the preparation process. The binding site was defined by the position of the pocket containing the co-crystallized ligand.

4.6. Ligand Preparation

340 UA derivatives in our in-house database (Supplementary Table S1) were retrieved from our previous publication [19] and constructed by utilizing the ChemDraw professional software to generate a two-dimensional (2D) shape of all compounds. For each compound, a proper complexation condition was created when creating conformations of low energy rings at the standard pH range of 5.0–9.0. At the CHARMm force field, the topology was optimized/utilizing the conjugate gradient approach, with divergence gradients of 0.1 kcal/mol, 0.01 kcal/mol, and 0.001 kcal/mol, respectively [33]. The produced two-dimensional (2D) structural molecules were decided to be encoded to three-dimensional (3D) format and equipped for docking study using DS3.1 and the CHARMm force field. Throughout the docking investigation, the randomized conformational number was set to 10. The co-crystallized compounds of proteins were employed as reference compounds.

4.7. Molecular Docking with Selected Compounds

In the docking studies, the receptor was designated as the pre-prepared protein model, and the binding site was identified as the location of the co-crystallized ligand found in the crystal structure. In this virtual screening study, the values acquired for the protein-co-crystallized ligand complex were used as the reference.

The CHARMm force field is used by the CDOCKER in DS3.1 [34], which uses grid-based molecular docking to allow numerous ligands to dock against a single protein receptor. The grid box consisted of 0.31 Å× -29.21 Å× -15.09 Å points around the active region, with an available grid spacing of 9.10 Å, with other parameters set as default. During the refining, it keeps the receptor stiff while allowing the ligands to be flexible. High-temperature molecular dynamics is used to create the random ligand conformations, which are then followed by random rotations to imitate annealing and complete force field reduction.

Binding energy was determined in kcal/mol, with lower values indicating stronger interactions between the ligand and the protein. Using DS3.1, the 2D and 3D interaction forms of the docked complex were utilized to detect amino acids present in the ligand–protein binding site. The computed binding energy of the ligand-target complex was used to rank 23 UA derivatives that were docked into the receptor model. The top hits were chosen based on their binding energies being higher (more negative) or comparable to that of a co-crystallized ligand when in combination with the receptor.

4.8. ADMET Prediction

The ADMET profile may be used to estimate potential and safety before it is placed on the market through absorption, distribution, metabolism, excretion, and toxicity. Unwanted property compounds frequently increase costs and cause significant stress in patients [35]. Consequently, it is essential to forecast ADMET characteristics during hit detection and optimization. Consequently, forecasting ADMET characteristics throughout hit identification and improvement is critical. The ADMET properties of the tested compounds were determined using the DS3.1 programme. The Chemistry at CHARMm (Harvard Macromolecular Mechanics) force field was used first, followed by the production and minimization of the compounds using the formulation for tiny compounds procedure. The ADMET properties technique was then used to carry out these tests using the DS3.1 software's "**Small Molecules**" option.

4.9. Drug-likeness Properties

The Molinspiration Cheminformatics server (http://www.molinspiration.com) was utilized to evaluate the bioactivity score of chosen compounds. Large chemical databases are evaluated in this computational chemistry approach in order to uncover potential novel medication candidates. This computational chemistry method scours a huge number of chemical databases in search of potential new drug candidates [36]. The Molinspiration program's miscreen engine evaluates drug ingredients against inactive substances, utilizing strong Bayesian statistics after analyzing a training set of active configurations (in extreme situations, even though a single active substance is important to produce a functional design). It is just essential to know the SMILES or SD file structures of active substances; no knowledge of the active region or binding complex is needed. The nine descriptors include log-P, topological polar surface area, molecular weight, number of atoms, number of ON, number of ONH, number of violations, number of rotatable bonds, and volume to Lipinski's rule.

4.10. CYP Isoform Study

SwissADME (http://www.swissadme.ch) software was used to investigate additional variables that influence drug digestion within the body [18].The cytochrome P450 enzyme (CYP) was also investigated, particularly a CYP inhibitor. This forecaster is part of the isozyme family, which is involved in drug biotransformation. Using the SwissADME online software, the presence of a CYP inhibitor was determined by entering the code yes for inhibitor presence and no for non-inhibitor absence. For a compound, if it shows a *yes* code, it was eliminated in the post-analysis process.

Medication metabolism through CYP is critical for a variety of drug interactions in the body, which can lead to toxicity, diminished pharmacological properties, and horrible drug reactions. Inputting molecules to be assessed for ADME, physicochemistry, drug-likeness, pharmacokinetics, and medicinal chemistry friendly qualities on http://www.swissadme.ch in a web browser brings up the SwissADME submission page [18]. The real input for computation is this list, which may be found on the right-hand side of the submission page. It may be modified like any other text, and SMILES can be typed or pasted. One input molecule per line is characterized by a SMILES and optionally a name separated by a space in the list. If the name field is left blank, SwissADME will generate an identity for you. It's worth noting that both the buttons for transferring the drawing to the SMILES list and conducting the computation are dynamic, meaning they'll only work if the operation is possible.

4.11. Molecular Dynamic (MD) Simulation

MD simulations was carried out to comprehend the dynamic behavior of the examined IV A protein and compound-4 dietary components under a time-dependent microcanonical ensemble. The structural behavior of food substances linked to the IV A protein in dynamic states was specifically investigated using an all-atoms conventional MD simulation during a time span of 50 ns. The full MD simulation was carried out using the Amber20 software [37] package loaded on a Linux operating system environment with a system configuration of 10th Generation Intel Core i9-10885H and NVIDIA® GeForce RTXTM 2070. The IV A protein and the compound-complex was encapsulated in the truncated octahedron of the TIP3P water model [38]. In order to neutralize the complicated system and keep the system's ionic strength at 0.1 M while simulating, an appropriate or necessary amount of Na$^+$ and Cl$^-$ were also injected to the entire system. The force fields ff14SB and GAFF2, respectively [39] were used to create the topology files for protein and small molecule. The simulation execution was carried out using the pmemd.cuda module of Amber20. A Langevin thermostat kept the temperature of the entire protein-ligand system at 300K. The Monte Carlo barostat was used to adjust the collision frequency to 2 ps-1 at 1 atm [38]. The covalent bonds connected with hydrogen atoms were restricted using the SHAKE algorithm. The eight threshold was used to address short-range electrostatic interactions, and the particle mesh Ewald approach was used to address long range electrostatic interactions [40]. Prior to the start of simulation production, the solvent and ions were equilibrated over a 10 ns time period utilizing NVT and NPT ensembles [41]. A number of trajectories analyzing parameters, including RMSD, root-mean-square fluctuation (RMSF), radius of gyration (RoG) and an entire hydrogen bond interaction profile, were estimated from the entire simulation trajectories after the MD simulation run was complete in order to investigate the stability of all protein-ligand complex.

1035

Miah et al.

Pharmacophore-based Molecular Docking of Usnic Acid Derivatives to Discover Anti-viral drugs Against Influenza A Virus

Journal of Research in Pharmacy

Research Article

REFERENCES

[1] Birch L, Murray CW, Hartshorn MJ, Tickle IJ, Verdonk ML. Sensitivity of molecular docking to induced fit effects in influenza virus neuraminidase. J Comput Aided Mol Des. 2002; 16(12): 855-869. https://doi.org/10.1023/A:1023844626572

[2] Ferro S, Gitto R, Buemi MR, Karamanou S, Stevaert A, Naesens L, De Luca L. Identification of influenza PA-Nter endonuclease inhibitors using pharmacophore-and docking-based virtual screening. Bioorg Med Chem. 2018; 26(15): 4544-4550. https://doi.org/10.1016/j.bmc.2018.07.046.

[3] Ye J, Yang X, Xu M, Chan PKS, Ma C. Novel N-Substituted oseltamivir derivatives as potent influenza neuraminidase inhibitors: Design, synthesis, biological evaluation, ADME prediction and molecular docking studies. Eur J Med Chem. 2019; 182: 111635. https://doi.org/10.1016/j.ejmech.2019.111635.

[4] Makau JN, Watanabe K, Ishikawa T, Mizuta S, Hamada T, Kobayashi N, Nishida N. Identification of small molecule inhibitors for influenza a virus using in silico and in vitro approaches. PloS One. 2017; 12(3): e0173582. https://doi.org/10.1371/journal.pone.0173582.

[5] Sadati SM, Gheibi N, Ranjbar S, Hashemzadeh MS. Docking study of flavonoid derivatives as potent inhibitors of influenza H1N1 virus neuraminidase. Biomed Rep. 2019; 10(1): 33-38. https://doi.org/10.3892%2Fbr.2018.1173.

[6] Basha SH, Prasad RN. In-Silico screening of Pleconaril and its novel substituted derivatives with Neuraminidase of H1N1 Influenza strain. BMC Res Notes. 2012; 5: 105. https://doi.org/10.1186%2F1756-0500-5-105.

[7] Gansukh E, Anthonydhason V, Jung S, Kim DH, Muthu M, Gopal J, Chun S. Nanotherapeutic anti-influenza solutions: current knowledge and future challenges. J Clust Sci. 2018; 29(6): 933-941. https://doi.org/10.1007/s10876-018-1417-z.

[8] Ingolfsdottir K. Usnic acid. Phytochem. 2002; 61(7): 729-736. https://doi.org/10.1016/S0031-9422(02)00383-7

[9] Sokolov DN, Zarubaev VV, Shtro AA, Polovinka MP, Luzina OA, Komarova NI, Kiselev OI. Anti-viral activity of (−)-and (+)-usnic acids and their derivatives against influenza virus A (H1N1) 2009. Bioorg Med Chem Lett. 2012; 22(23): 7060-7064. https://doi.org/10.1016/j.bmcl.2012.09.084.

[10] Cocchietto M, Skert N, Nimis P, Sava G. A review on usnic acid, an interesting natural compound. Naturwissenschaften. 2002; 89(4): 137-146. https://doi.org/10.1007/s00114-002-0305-3

[11] Bomfim RR, Araujo AA, Cuadros-Orellana S, Melo MG, Quintans-Junior LJ, Cavalcanti SC, de Bioprocessos LDE. Larvicidal activity of *Cladonia substellata* extract and usnic acid against *Aedes aegypti* and *Artemia salina*. Lat Am J Pharm. 2009; 28(4): 580-584.

[12] Shtro AA, Zarubaev VV, Luzina OA, Sokolov DN, Kiselev OI, Salakhutdinov NF. Novel derivatives of usnic acid effectively inhibiting reproduction of influenza A virus. Bioorg Med Chem. 2014; 22(24): 6826-6836. https://doi.org/10.1016/j.bmc.2014.10.033.

[13] Stephanie F, Saragih M, Alkaff AH, Nasution MAF, Tambunan USF. Screening of potential Northern African natural product compounds as Dengue Virus NS5 Methyltransferase Inhibitor: An in silico approach. In 2019 IEEE 19th Int Confer Bioinfor Bioeng (BIBE). 2019; 215-220. https://doi.org/10.1109/BIBE.2019.00046

[14] Fudo S, Yamamoto N, Nukaga M, Odagiri T, Tashiro M, Hoshino T. Two distinctive binding modes of endonuclease inhibitors to the N-terminal region of influenza virus polymerase acidic subunit. Biochem. 2016; 55(18): 2646-2660. https://doi.org/10.1021/acs.biochem.5b01087.

1036

Miah et al.
Pharmacophore-based Molecular Docking of Usnic Acid Derivatives to Discover Anti-viral drugs Against Influenza A Virus

Journal of Research in Pharmacy

Research Article

[15] Colmenarejo G, Alvarez-Pedraglio A, Lavandera JL. Cheminformatic models to predict binding affinities to human serum albumin. J Med Chem. 2001; 44(25): 4370-4378. https://doi.org/10.1021/jm010960b.

[16] Singh J, Kumar M, Mansuri R, Sahoo GC, Deep A. Inhibitor designing, virtual screening, and docking studies for methyltransferase: a potential target against dengue virus. J Pharm Bioallied Sci. 2016; 8(3): 188-194. https://doi.org/10.4103%2F0975-7406.171682.

[17] Lipinski CA. Lead-and drug-like compounds: the rule-of-five revolution. Drug Dis Today: Technol. 2004; 1(4): 337-341. https://doi.org/10.1016/j.ddtec.2004.11.007

[18] Daina A, Michielin O, Zoete V. SwissADME: A free web tool to evaluate pharmacokinetics, drug-likeness and medicinal chemistry friendliness of small molecules. Sci Rep. 2017; 7(1): 42717. https://doi.org/10.1038/srep42717.

[19] Roney M, Huq AM, Rullah K, Hamid HA, Imran S, Islam MA, Mohd Aluwi MFF. Virtual screening-based identification of potent DENV-3 RdRp protease inhibitors via In-House usnic acid derivative database. J Comput Biophy Chem. 2021; 20(8): 797-814. https://doi.org/10.1142/S2737416521500496.

[20] Go RE, Hwang KA, Choi KC. Cytochrome P450 1 family and cancers. J Steroid Biochem Mol Biol. 2015; 147: 24-30. https://doi.org/10.1016/j.jsbmb.2014.11.003.

[21] Cribb AE, Peyrou M, Muruganandan S, Schneider L. The endoplasmic reticulum in xenobiotic toxicity. Drug Metabol Rev. 2005; 37(3): 405-442. https://doi.org/10.1080/03602530500205135

[22] Roy M, Datta A. (2019). Pharmacogenomics and Phytochemicals. In: Cancer Genetics and Therapeutics. Springer, Singapore. https://doi.org/10.1007/978-981-13-9471-3_7.

[23] Ogu CC, Maxa JL. Drug interactions due to cytochrome P450. Proc (Baylr Univ Med Cent). 2000; 13(4): 421-423. https://doi.org/10.1080%2F08998280.2000.11927719

[24] Bibi Z. Role of cytochrome P450 in drug interactions. Nutr Metabol (London). 2008; 5: 27. https://doi.org/10.1186%2F1743-7075-5-27.

[25] Bagastama AR, Alkaff AH, Tambunan USF. Discovery of natural product compounds as Dengue Virus NS5 Methyltransferase Inhibitor candidate through in silico method. Key Engineer Mater. 2020; 840: 270-276. https://doi.org/10.4028/www.scientific.net/KEM.840.270.

[26] Nebert DW, Russell DW. Clinical importance of the cytochromes P450. The Lancet. 2002; 360(9340): 1155-1162. https://doi.org/10.1016/S0140-6736(02)11203-7

[27] Siegle I, Fritz P, Eckhardt K, Zanger UM, Eichelbaum M. Cellular localization and regional distribution of CYP2D6 mRNA and protein expression in human brain. Pharmacogenet. 2001; 11(3): 237-245. https://doi.org/10.1097/00008571-200104000-00007.

[28] Tripathi N, Goel B, Bhardwaj N, Sahu B, Kumar H, Jain SK. Virtual screening and molecular simulation study of natural products database for lead identification of novel coronavirus main protease inhibitors. J Biomol Struct Dyn. 2022; 40(8): 3655-3667. https://doi.org/10.1080/07391102.2020.1848630.

[29] El Bakri Y, Anouar EH, Ahmad S, Nassar AA, Taha ML, Mague JT, Essassi EM. Synthesis and identification of novel potential molecules against COVID-19 main protease through structure-guided virtual screening approach. Appl Biochem Biotechnol. 2021; 193(11): 3602-3623. https://doi.org/10.1007/s12010-021-03615-8.

[30] Aldahham BJ, Al-Khafaji K, Saleh MY, Abdelhakem AM, Alanazi AM, Islam MA. Identification of naphthyridine and quinoline derivatives as potential Nsp16-Nsp10 inhibitors: A pharmacoinformatics study. J Biomol Struct Dyn.2022; 40(9): 3899-3906. https://doi.org/10.1080/07391102.2020.1851305.

[31] Zhang L, Yang L, Li R T, Yu F, Zhong J. A new prenylated 3-benzoxepin derivative with anti-influenza A virus activity from *Elsholtzia penduliflora*. Nat Prod Res. 2020; 1-7. https://doi.org/10.1080/14786419.2020.1799360.

[32] Balaramnavar VM, Ahmad K, Saeed M, Ahmad I, Kamal M, Jawed T. Pharmacophore-based approaches in the rational repurposing technique for FDA approved drugs targeting SARS-CoV-2 Mpro. RSC Adv. 2020; 10(66): 40264-40275. http://xlink.rsc.org/?DOI=d0ra06038k.

[33] Chen J, Jiang H, Li F, Hu B, Wang Y, Wang M, Cheng M. Computational insight into dengue virus NS2B-NS3 protease inhibition: A combined ligand-and structure-based approach. Comput Biol Chem. 2018; 77: 261-271. https://doi.org/10.1016/j.compbiolchem.2018.09.010.

[34] Aluwi MFFM, Rullah K, Haque MA, Yamin BM, Ahmad W, Amjad MW, Lam KW. Suppression of PGE 2 production via disruption of MAPK phosphorylation by unsymmetrical dicarbonyl curcumin derivatives. Med Chem Res. 2017; 26(12): 3323-3335. https://doi.org/10.1007/s00044-017-2025-4.

1037

Miah et al.

**Pharmacophore-based Molecular Docking of Usnic Acid Derivatives
to Discover Anti-viral drugs Against Influenza A Virus**

Journal of Research in Pharmacy

Research Article

[35] Razzaghi-Asl N, Mirzayi S, Mahnam K, Sepehri S. Identification of COX-2 inhibitors via structure-based virtual screening and molecular dynamics simulation. J Mol Graph Mod. 2018; 83: 138-152. https://doi.org/10.1016/j.jmgm.2018.05.010.

[36] Mishra SS, Sharma CS, Singh HP, Pandiya H, Kumar N. In silico ADME, Bioactivity and toxicity parameters calculation of some selected anti-tubercular drugs. Int J Pharmacol Phytopharmacol Res. 2016; 6: 77-79. https://doi.org/10.24896/eijppr.2016661.

[37] Atatreh N, Hasan S, Ali BR, Ghattas MA. Computer-aided approaches reveal trihydroxychroman and pyrazolone derivatives as potential inhibitors of SARS-CoV-2 virus main protease. Acta Pharm. 2021; 71(3): 325-333. http://dx.doi.org/10.2478/acph-2021-0040.

[38] Bhowmick S, Saha A, AlFaris NA, ALTamimi JZ, ALOthman ZA, Aldayel TS, Islam MA. Identification of potent food constituents as SARSCoV-2 papain-like protease modulators through advanced pharmacoinformatics approaches. J Mol Graph Mod. 2022; 111: 108113. https://doi.org/10.1016/j.jmgm.2021.108113

[39] Luzik DA, Rogacheva ON, Izmailov SA, Indeykina MI, Kononikhin AS, Skrynnikov NR. Molecular dynamics model of peptide-protein conjugation: Case study of covalent complex between Sos1 peptide and N terminal SH3 domain from Grb2. Sci Rep. 2019; 9: 20219. https://doi.org/10.1038/s41598-019-56078-7.

[40] Kalé L, Skeel R, Bhandarkar M, Brunner R, Gursoy A, Krawetz N, Schulten K. NAMD2: greater scalability for parallel molecular dynamics. J Comput Phys. 1999; 151(1): 283-312. https://doi.org/10.1006/jcph.1999.6201

[41] Basdevant N, Dessaux D, Ramirez R. Ionic transport through a protein nanopore: a Coarse-Grained Molecular Dynamics Study. Sci Rep. 2019; 9: 15740. https://doi.org/10.1038%2Fs41598-019-51942-y.